Near-field optical microscopy of surface plasmon polaritons excited by silicon nanoantenna

I. S. Sinev, F. E. Komissarenko, I. S. Mukhin, M. I. Petrov, I. V. Iorsh, P. A. Belov, A. K. Samusev

St. Petersburg National Research University of Information Technologies,
Mechanics and Optics,
Kronverkskiy, 49, St. Petersburg, 197101, Russia

i.sinev@metalab.ifmo.ru

An optical nanoantenna is a device that transforms far-field electromagnetic radiation into near-field and vice versa. Naturally, it can serve as a conduit between free space light and localized optical modes, including surface waves. With the recent rise of all-dielectric nanophotonics, nanoantennas made of high-index materials were found to offer unparalleled means for manipulation of light due to presence of equally strong electric and magnetic responses in the visible spectral range. Here, we demonstrate excitation of surface plasmon polaritons by single silicon nanosphere on gold layer measured by means of scanning near-field optical microscopy. The interference patterns observed in the measured near-field maps allow us to retrieve information on directivity and relative excitation efficiency of surface plasmon polariton in the longer wavelength part of the visible spectral range. Our results demonstrate that all-dielectric nanoantennas could prove to be a valuable tool for controlling directivity and efficiency of excitation of surface waves.

Keywords: near-field optical microscopy, silicon nanoparticles, all-dielectric nanoantennas, surface plasmon polaritons.

Received: 13 September 2018

1. Introduction

Within the last decade, all-dielectric nanophotonics established itself as a viable alternative for plasmonics due to lower losses and additional opportunities for light manipulation due to possibility of achieving non-unitary effective magnetic permeability. The concept of all-dielectric nanoantennas for the visible spectral range became reality with the discovery of strong scattering resonances of silicon nanospheres of 100 – 200 nm size [1, 2]. Initially, the studies of high-index nanoantennas for the visible range were mainly focused on the operation with bulk electromagnetic waves. A number of fascinating effects stemming from interference of equally strong electric and magnetic dipole resonances were discovered since then. Those are directional scattering of light [3], generalized Brewster effect [4], etc. At the same time, the performance of high-index nanoantennas in the domain of surface waves remained mostly unexplored with a few exceptions [5].

Here, we demonstrate that resonant silicon nanoparticle on metal film can act as an effective nanoantenna that converts free space light into surface plasmon polaritons. We visualize the excitation of SPP from silicon nanosphere on gold film using scanning near-field optical microscopy with aperture-type probe. In the near-field maps measured for oblique incidence of linearly polarized laser beam on the nanosphere, the surface wave excitation is manifested due to interference with the incident wave. We show that the obtained near-field maps can be used to retrieve information on directivity of excited surface plasmon polariton and compare the SPP excitation efficiency for s- and p-polarized light.

2. Methods

Resonant silicon nanoparticles were fabricated using laser ablation from thin films of amorphous silicon on glass following a well-established routine [6]. The ablation was performed using Yb^{3+} femtosecond laser (Avesta TeMa-150). Nanoparticles deposited back on silicon film were then transferred to 200 nm layer of crystalline gold using nanoscale manipulations under an electron beam [7].

The scheme of experimental setup for mapping the near-field of silicon nanoantenna on gold is shown in Fig. 1(a). The nanoparticle is excited with mildly focussed linearly polarized laser beam incident at $\theta \approx 65$ degrees. During the experiment, the near-field probe represented by a tapered metallized optical fiber with a subwavelength (100 nm) aperture at its tip is scanned within a plane at a fixed distance from the sample surface. As compared to standard regime with shear-force feedback, this regime allows one to avoid artifacts of near-field signal close to the sphere as well as accidental displacement of the sphere during the scan. Signal collected with the near-field probe was measured with photomultiplier tube (Hamamatsu H10792) in lock-in detection scheme.
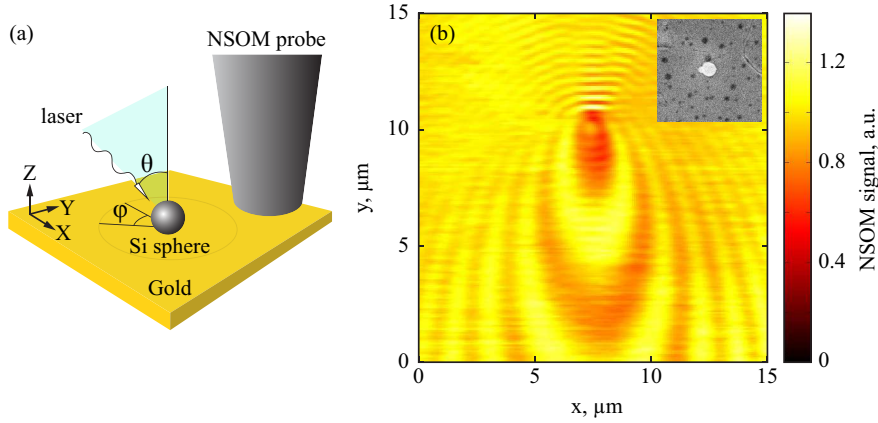
FIG. 1. (a) Sketch of the scanning near-field optical microscopy of surface plasmon polariton from silicon nanoantenna on gold. (b) Near-field map of resonant 200 nm silicon nanoantenna on gold excited with laser beam at a wavelength of 780 nm. The inset shows SEM image of silicon nanoantenna on gold

To study the spectral dependence of the near-field maps of surface plasmon polariton excited with the silicon nanosphere, we employed supercontinuum laser source (Fianium WhiteLase SC400-6) with tunable filter (Fianium SuperChrome). The central wavelength of the beam yielded by the system was tuned within 600 – 800 nm spectral range, while the bandwidth of the beam was 10 nm.

Theoretical modelling of the optical properties of silicon nanosphere on gold was performed using analytical model based on Green function approach [8]. Within this model, silicon nanosphere is described as a superposition of point electric and magnetic dipoles placed in its center. The corresponding electric and magnetic polarizabilities of the nanoparticle are first calculated using Mie theory [9] and then renormalized with account for the influence of the substrate as described elsewhere [8]. Using the calculated polarizabilities, it is then possible to find both the far-field scattering cross section of the particle and the fields of the SPP excited by the particle. The angular dependence of the intensity of the excited SPP wave is described by the formula [10]:

$$I_{SPP} \sim \left| \cos\varphi(m_y - i\kappa p_x) - \tilde{k}_{SPP}p_z \right|^2, \tag{1}$$

where φ is the direction of SPP excitation with respect to the plane of incidence, m_y and p_x are in-plane (parallel to the substrate) components of magnetic and electric polarizability of the nanosphere, and p_z is electric dipole component oriented normally to the substrate. $\tilde{k}_{SPP} = \sqrt{\varepsilon_m/(\varepsilon_m + 1)}$ stands for the normalized wavevector of the SPP on the interface of air and metal with dielectric permittivity ε_m, while $\kappa = -i\sqrt{1/(\varepsilon_m + 1)}$ characterizes the SPP localization in the direction normal to the substrate.

3. Results and discussion

Surface plasmon polaritons are localized modes that propagate along the interface between dielectric and metallic materials. Therefore, they cannot be directly addressed with common far-field microscopy techniques, and auxiliary devices or structures are needed for their excitation and detection. Namely, the characteristics SPP are studied using prisms in frustrated total internal reflection geometry [11] or via grating couplers and decouplers that provide additional momentum required to match the wavevector of light with that of SPP. Another option is offered by near-field scanning optical microscopy (NSOM), which allows to directly probe the evanescent components of SPP field. In this case, the parameters of SPP waves, such as wavelength and directivity, are manifested through near-field interference. For example, in case of scattering type NSOM, the surface waves are characterized using standing wave pattern that forms due to interference of surface waves launched by the probe and reflected from the sample edges or other defects [12]. In case of aperture-type NSOM, which detects free-space radiation as well, the excitation of surface plasmon polariton can be detected through interference with the incident wave. For example, in work by Permyakov *et al.* [13] the measured near-field maps of a hole in silver film manifested double-lobe interference pattern characteristic for SPP excited with a point magnetic dipole, which in that case was represented by the subwavelength hole in metal film [14].
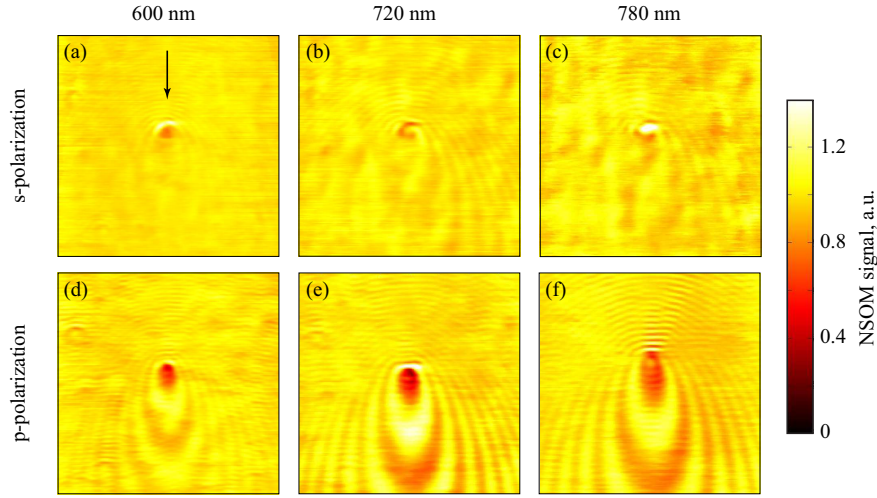
FIG. 2. Measured NSOM maps of SPP from 200 nm silicon nanosphere for three different wavelengths for s-polarization (a–c) and p-polarization (d–f). The size of each image is $15 \times 15 \ \mu m^2$. The direction of incident light is shown with an arrow in panel (a)

In the experimental configuration used in our work, due to non-zero angle of incidence of the excitation beam the period of the observed interference pattern, T depends on the azimuthal angle (see characteric maps in Fig. 1b and Fig. 2). This dependence can be described with a simple formula:

$$T(\varphi) = \frac{2\pi}{k_0 \sin\theta \cos\varphi + k_{SPP}}, \tag{2}$$

where θ stands for the angle of incidence, φ is the azimuthal angle, and $k0, k_{SPP}$ are the wavevectors of free space light and SPP, respectively (see also Fig. 1a). Another factor affecting the near-field maps is the azimuthal dependence of the SPP excitation efficiency, which defines the relative amplitude of the modulation in a given direction and can be evaluated using eq. 1. Finally, total SPP excitation efficiency governs the maximum modulation depth of the interference pattern.

Fig. 2 shows the near-field maps of a 200 nm silicon nanosphere on gold substrate measured for s- and p-polarized incident light with wavelengths within 600-800 nm spectral range. As the figure clearly shows, the maps for different polarizations demonstrate different interference patterns. For p-polarized excitations, the maximum modulation is observed in forward direction. At the same time, for s-polarization the modulation is much weaker and is virtually suppressed in forward and backward directions. At the same time, for the same polarization the modulation depth increases towards 780 nm wavelength. These features can be explained using the formula for SPP intensity, eq. 1. First, it reveals that for s-polarized light, SPP is not excited in forward and backward directions as both p_y and m_x dipole moments contributing to SPP in such configuration do not couple to SPP along the x-axis. Moreover, the SPP intensity is much higher for p-polarized excitation. Indeed, m_y and p_z momenta induced in the sphere excited with p-polarized light couple to SPP with much higher efficiency (factors of 1 and $\tilde{k}_{SPP}$, respectively, the latter being close to unity in the considered spectral range [15]). On the contrary, coupling of p_y moment induced for s-polarization into SPP is suppressed by a factor of $1/\kappa \sim \sqrt{\varepsilon_m + 1}$, which reaches 5 – 7 for gold in the same spectral range. The observed spectral maximum of the SPP excitation efficiency corresponds to the onset of magnetic dipole resonance of the sphere (m_y). The contribution of electric dipole to SPP p_z is non-resonant, as it was demonstrated in our earlier work [16].

Finally, to retrieve the information on the directivity of excited SPP from the measured maps, we performed Fourier transform of the experimental data represented in polar coordinates (r, φ), where r is the distance from the center of the sphere. The NSOM map for 780 nm excitation wavelength processed accordingly is shown in Fig. 3a. The map reveals angle-dependent maximum which corresponds to the inverse period of the interference pattern. Its position is in great agreement with the interference period calculated from eq. 2 with account for the dispersion of gold dielectric permittivity at a given wavelength [15]. The Fourier-transformed data also allows to reconstruct the directivity pattern of the excited SPP by plotting the angular dependence of the intesity of the peak corresponding to SPP. Directivity pattern reconstructed from the NSOM data for 780 nm excitation is shown in Fig. 3b.
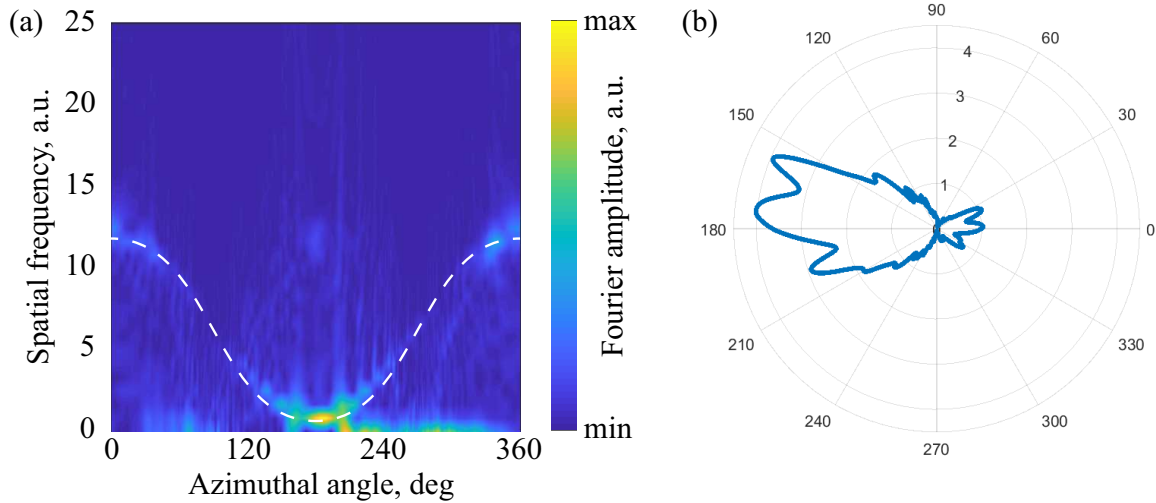
FIG. 3. (a) Fourier transform of NSOM map measured at 780 nm represented in polar coordinates. The dashed line represents the angular dependence of the period of interference pattern analytically calculated from eq. 2. (b) SPP directivity pattern reconstructed from (a)

Here, it is important to mention that the backward directivity of SPP retrieved from NSOM maps measured in such configuration is slightly underestimated due to the dependence of the excitation efficiency on the position of NSOM probe. Indeed, whenever the near-field probe moves into the "backward" half-space (top part of the maps in Fig. 1b and Fig. 2), it shades the nanosphere from the incident light, thus decreasing the effective amplitude of the incident wave at the nanosphere. Another factor influencing the reconstructed pattern is different data sampling for different angles due to changes in the period of the interference.

4. Conclusion

To conclude, in this work, we studied the surface plasmon polaritons excited by a resonant silicon nanosphere on gold film. The observed near-field maps exhibit signal modulation due to interference between the incident light and surface plasmon polariton excited from the silicon nanoantenna. The radial dependence of the interference fringes allowed us to evaluate the directivity pattern of the surface waves as well as their relative excitation efficiency. Our results show that single silicon nanoparticles can be used as compact yet effective antennas for directional excitation of surface plasmon polaritons.

Acknowledgements

References

[1] Evlyukhin A. B., Novikov S. M., Zywietz U., Eriksen R. L., Reinhardt C., Bozhevolnyi S. I., Chichkov B. N. Demonstration of magnetic dipole resonances of dielectric nanospheres in the visible region. *Nano letters*, 2012, **12**(7), P. 3749–3755.

[2] Kuznetsov A. I., Miroshnichenko A. E., Fu Y. H., Zhang J., LukYanchuk B. Magnetic light. *Scientific reports*, 2012, **2**, P. 492.

[3] Fu Y. H., Kuznetsov A. I., Miroshnichenko A. E., Yu Y. F., Lukyanchuk B. Directional visible light scattering by silicon nanoparticles. *Nature communications*, 2013, **4**, P. 1527.

[4] Paniagua-Domnguez R., Yu Y. F., Miroshnichenko A. E., Krivitsky L. A., Fu Y. H., Valuckas V., Gonzaga L., Toh Y. T., Kay A. Y. S., LukYanchuk B., Kuznetsov A. I. Generalized Brewster effect in dielectric metasurfaces. *Nature communications*, 2016, **7**, P. 10362.

[5] Evlyukhin A. B., Bozhevolnyi S. I. Resonant unidirectional and elastic scattering of surface plasmon polaritons by high refractive index dielectric nanoparticles. *Physical Review B*, 2015, **92**(24), P. 245419.

[6] Dmitriev P. A., Makarov S. V., Milichko V. A., Mukhin I. S., Gudovskikh A. S., Sitnikova A. A., Samusev A. K., Krasnok A. E., Belov P. A. Laser fabrication of crystalline silicon nanoresonators from an amorphous film for low-loss all-dielectric nanophotonics. *Nanoscale*, 2016, **8**(9), P. 5043–5048.

[7] Denisyuk A. I., Komissarenko F. E., Mukhin I. S. Electrostatic pick-and-place micro/nanomanipulation under the electron beam. *Microelectronic Engineering*, 2014, **121**, P. 15–18.

[8] Miroshnichenko A. E., Evlyukhin A. B., Kivshar Y. S., Chichkov B. N. Substrate-Induced Resonant Magnetoelectric Effects for Dielectric Nanoparticles. *ACS Photonics*, 2015, **2**(10), P. 1423–1428.

[9] Born M., Wolf E. *Principles of optics: electromagnetic theory of propagation, interference and diffraction of light*. Elsevier, 2013, 836 p.

[10] Sinev I. S., Bogdanov A. A., Komissarenko F. E., Frizyuk K. S., Petrov M. I., Mukhin I. S., Makarov S. V., Samusev A. K., Lavrinenko A. V., Iorsh I. V. Chirality driven by magnetic dipole response for demultiplexing of surface waves. *Laser & Photonics Reviews*, 2017, **11**(5), P. 1700168.

[11] Otto A. Excitation of nonradiative surface plasma waves in silver by the method of frustrated total reflection. *Zeitschrift fur Physik A Hadrons and nuclei*, 1968, **216**(4), P. 398–410.

[12] Woessner A., Lundeberg M. B., Gao Y., Principi A., Alonso-Gonzalez P., Carrega M., Watanabe K., Taniguchi T., Vignale G., Polini M., Hone J., Hillenbrand R., Koppens F. H. L. Highly confined low-loss plasmons in grapheneboron nitride heterostructures. *Nature materials*, 2015, **14**(4), P. 421.

[13] Permyakov D. V., Mukhin I. S., Shishkin I. I., Samusev A. K., Belov P. A., Kivshar Y. S. Mapping electromagnetic fields near a subwavelength hole. *JETP letters*, 2014, **99**(11), P. 622–626.

[14] Bethe H. A. Theory of diffraction by small holes. *Physical review*, 1944, **66**(7-8), P. 163.

[15] Johnson P. B., Christy R. W. Optical constants of the noble metals. *Physical review B*, 1972, **6**(12), P. 4370.

[16] Sinev I., Iorsh I., Bogdanov A., Permyakov D., Komissarenko F., Mukhin I., Samusev A., Valuckas V., Kuznetsov A. I., Luk'yanchuk B. S., Miroshnichenko A. E., Kivshar Y. S. Polarization control over electric and magnetic dipole resonances of dielectric nanoparticles on metallic films. *Laser & Photonics Reviews*, 2016, **10**(5), P. 799–806.